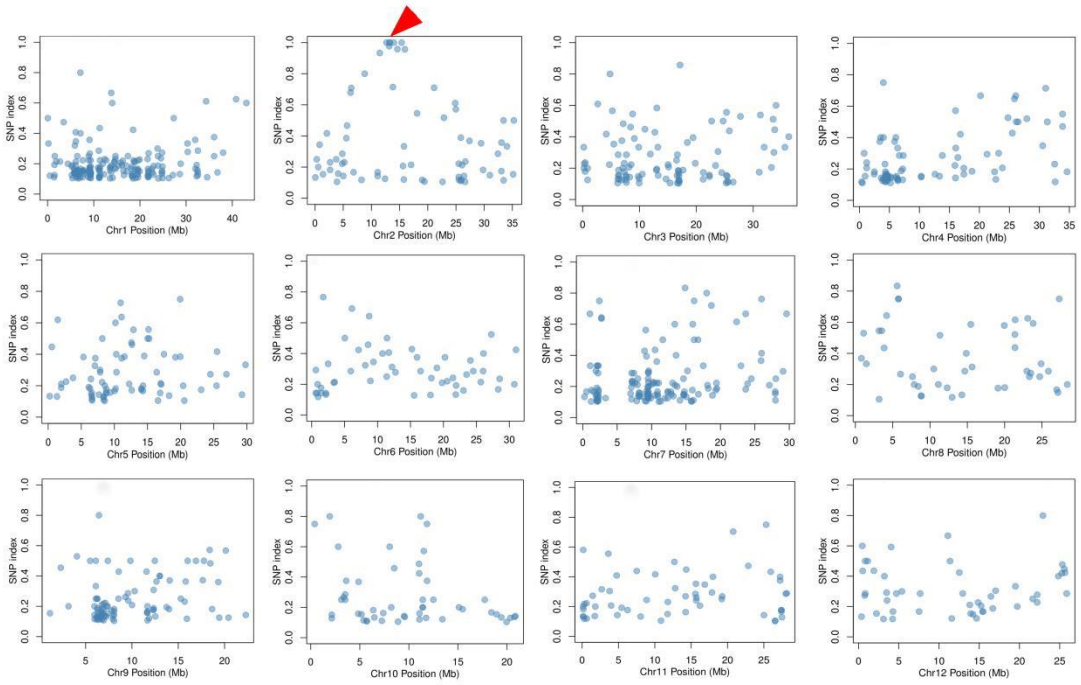

Figure S1. Distributions of SNP index along chromosomes.

The candidate *ap1* mutation on Chromosome 2 is indicated by a red arrow.

Figure S2. Protein sequence alignment of AP1 between the WT and *ap1*.

The sequences were displayed with BOXSHADE.

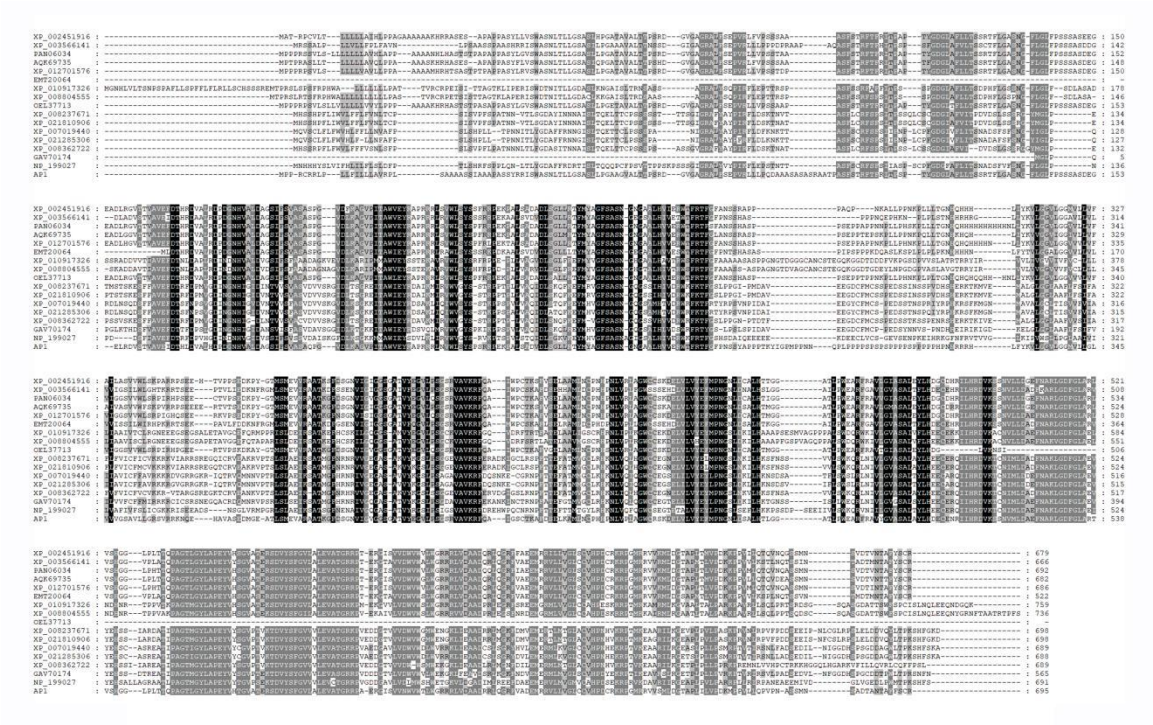

Figure S3. Protein sequences alignment of AP1 and its related homologs in other plant species.

The sequences were displayed with BOXSHADE.

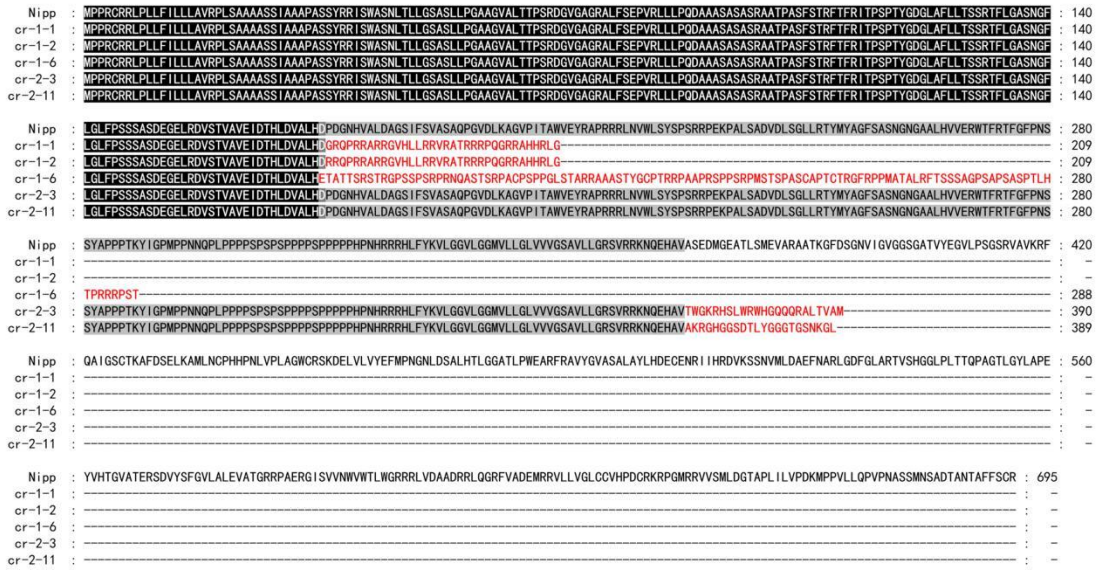

Figure S4. Protein sequences alignment of AP1 between Nipponbare (Nipp) and the CRISPR/Cas9-mediated (*cr*) mutants.

The sequences were displayed with BOXSHADE. The changed amino acids are highlighted by red color.

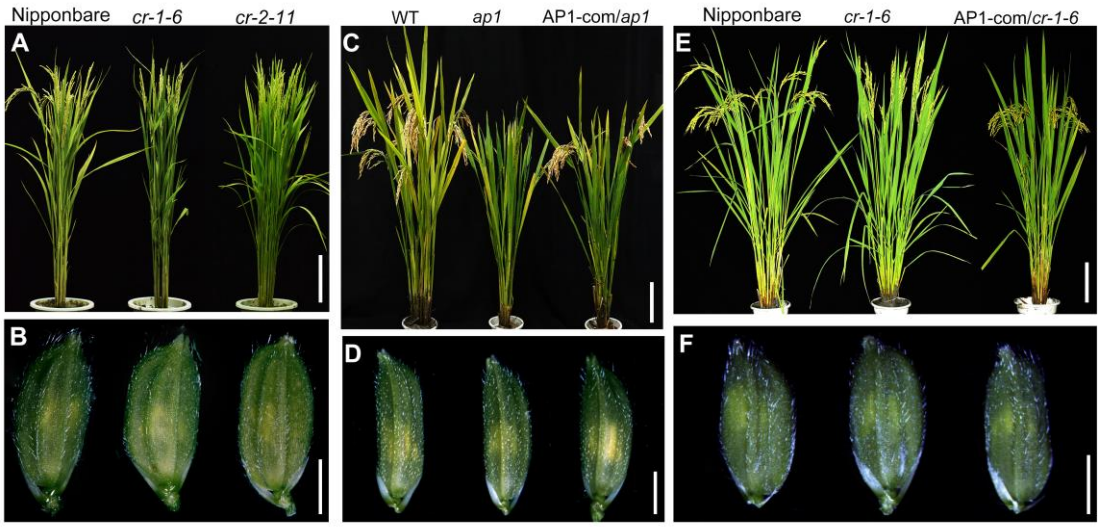

Figure S5. Phenotypic analysis of the CRISPR/Cas9-mediated (*cr*) mutants and the complemented lines.

(A) Mature plants of Nipponbare and the *cr* mutants. (B) Spikelets of Nipponbare and the *cr* mutants at heading stage. (C) Mature plants of the WT, *ap1* mutant and the complemented line (AP1-COM/*ap1*). (D) Spikelets of the WT, *ap1* mutant and the complemented line (AP1-COM/*ap1*) at heading stage. (E) Mature plants of Nipponbare, the *cr* mutant and the complemented line (AP1-COM/*cr-1-6*). (F) Spikelets of Nipponbare, the *cr* mutant and the complemented line (AP1-COM/*cr-1-6*) at heading stage. Scale bars: 15 cm (A, C, E); 2 mm (B, D, F).

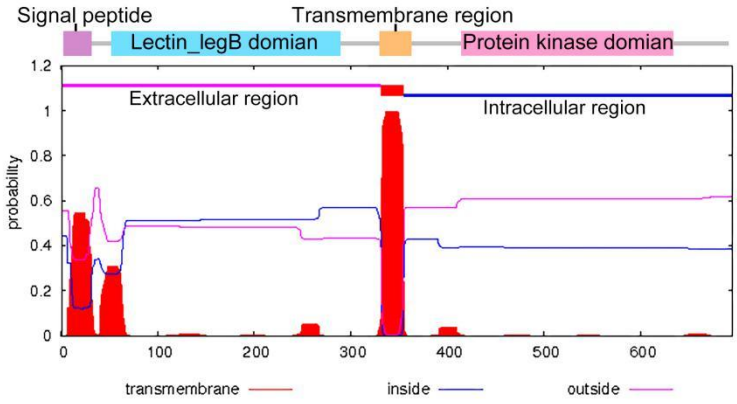

Figure S6. Subcellular localization of AP1 protein domains predicted by TMHMM 2.0.

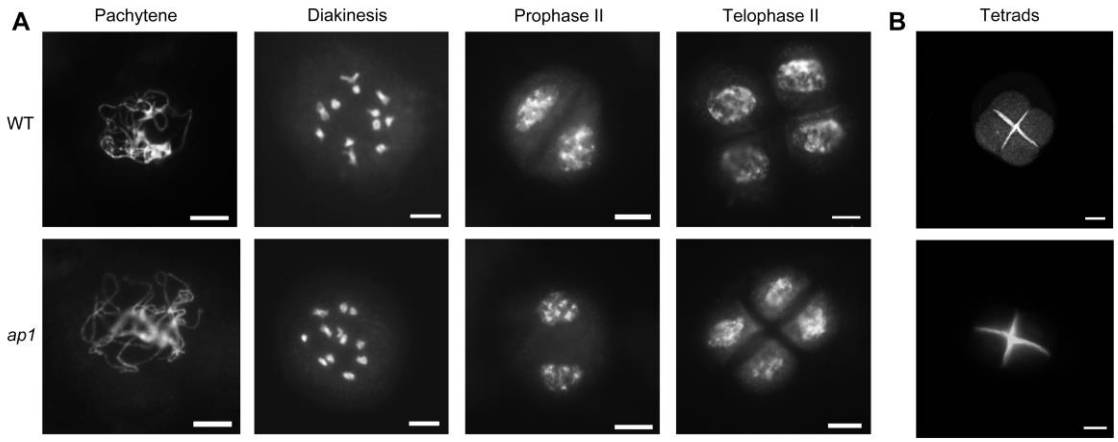

Figure S7. Meiotic processes in the WT and *ap1* anther.

(A) Chromosome behaviors in the WT (upper) and *ap1* (lower) during meiosis. (B) Callose wall of tetrads in the WT (upper) and *ap1* (lower). Scale bars: 10 μm.

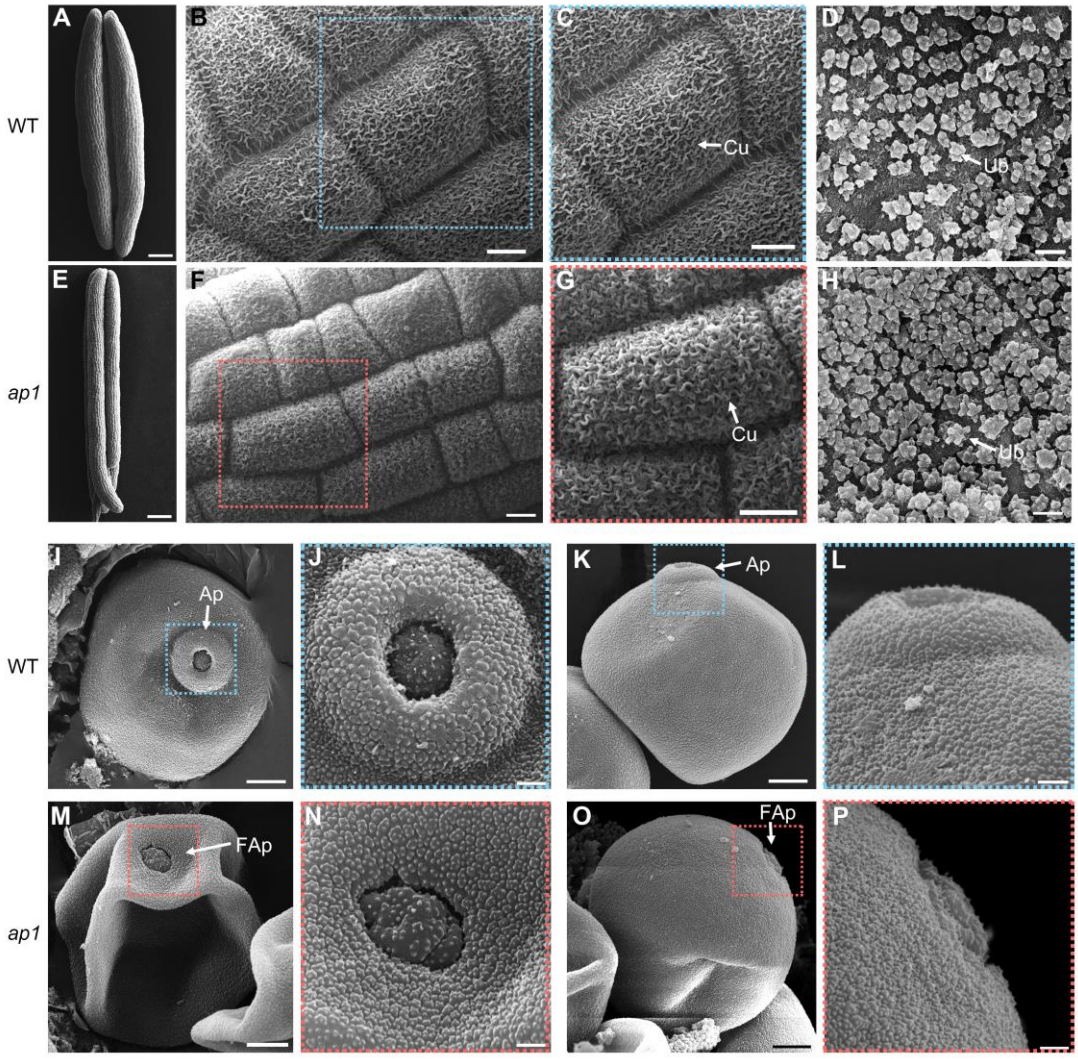

Figure S8. SEM analysis of anther and pollen in the WT and *ap1*.

(A-D, I-L) SEM analysis of the anther and pollen in the WT at stage 12. (E-H, M-P) SEM analysis of the anther and pollen in *ap1* at stage 12. (A, E) Anther. (B, F) Anther outer surface. (C, G) Enlarged images of the anther outer surface in (B) and (F), respectively. (D, H) Anther inner surface. (I, M) Top view of pollen grain. (J, N) Enlarged images of the aperture in (I) and (M), respectively. (K, O) Side view of pollen grain. (L, P) Enlarged images of the aperture in (K) and (O), respectively. Ap, aperture with annulus; Cu, cuticle; FAp, flat aperture lacking annulus. Scale bars: 200 μm (A, E); 10 μm (B, C, F, G); 1 μm (D, H, J, L, N, P); 5 μm (I, L, K, O).

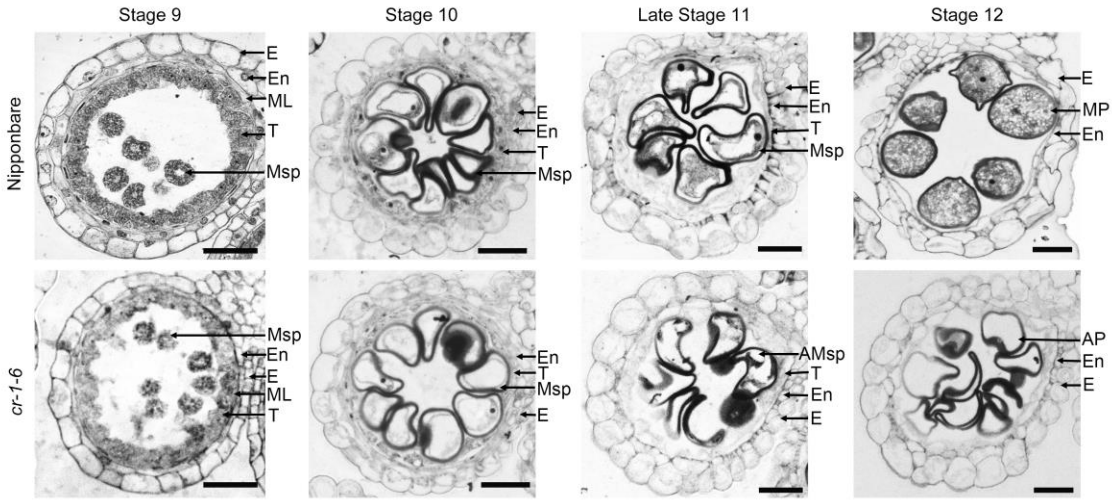

Figure S9. Transverse sections of anthers from Nipponbare (upper) and the CRISPR/Cas9-mediated (*cr*) mutants (lower) at different developmental stages.

AMsp, abnormal microspores; E, epidermis; En, endothecium; AP, abnormal pollen; ML, middle layer; MP, mature pollen; Msp, microspore; T, tapetum. Scale bars: 20 μm.

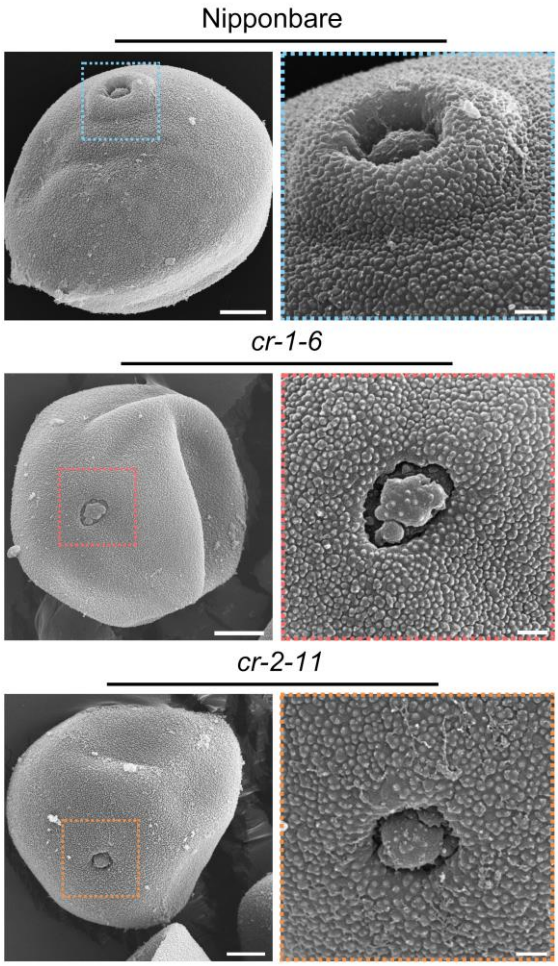

Figure S10. SEM analysis of pollen grains in Nipponbare and the CRISPR/Cas9-mediated (*cr*) mutants.

Enlarged images of the aperture were shown in right panels. Scale bars: 5 μm (the left panels); 1 μm (the right panels).

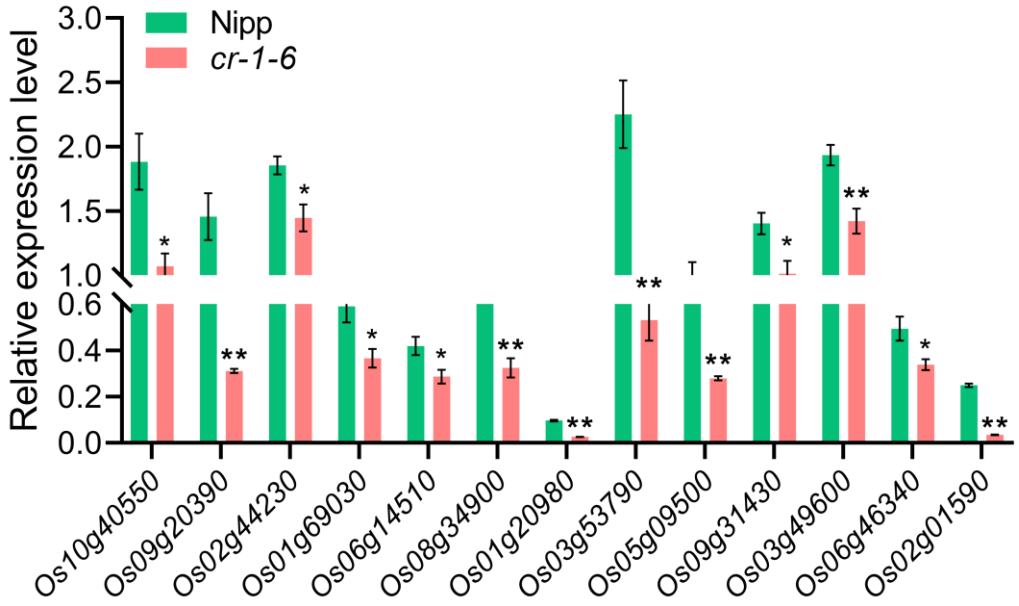

Figure S11. qRT-PCR analysis of several genes related to starch and sucrose metabolism in Fig. 8C

Spikelets of Nipponbare (Nipp) and the CRISPR/Cas9-mediated (*cr*) mutants during the anther stages 11 to 12 were analyzed. Values are means ± SEMof four biological replicates. * and **, statistical significance ($P < 0.05$ and $P < 0.01$) compared with Nipponbare using Student's *t*-test, respectively.

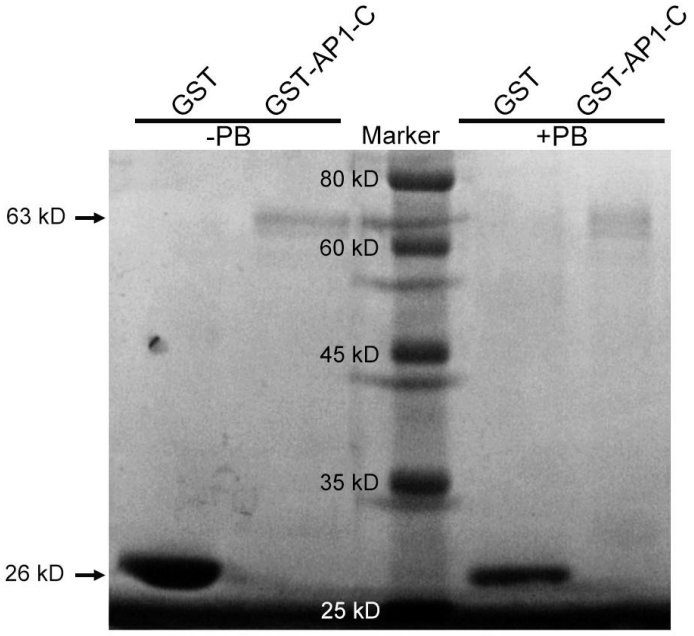

Figure S12. Detection of the recombinant proteins by Coomassie brilliant blue staining.

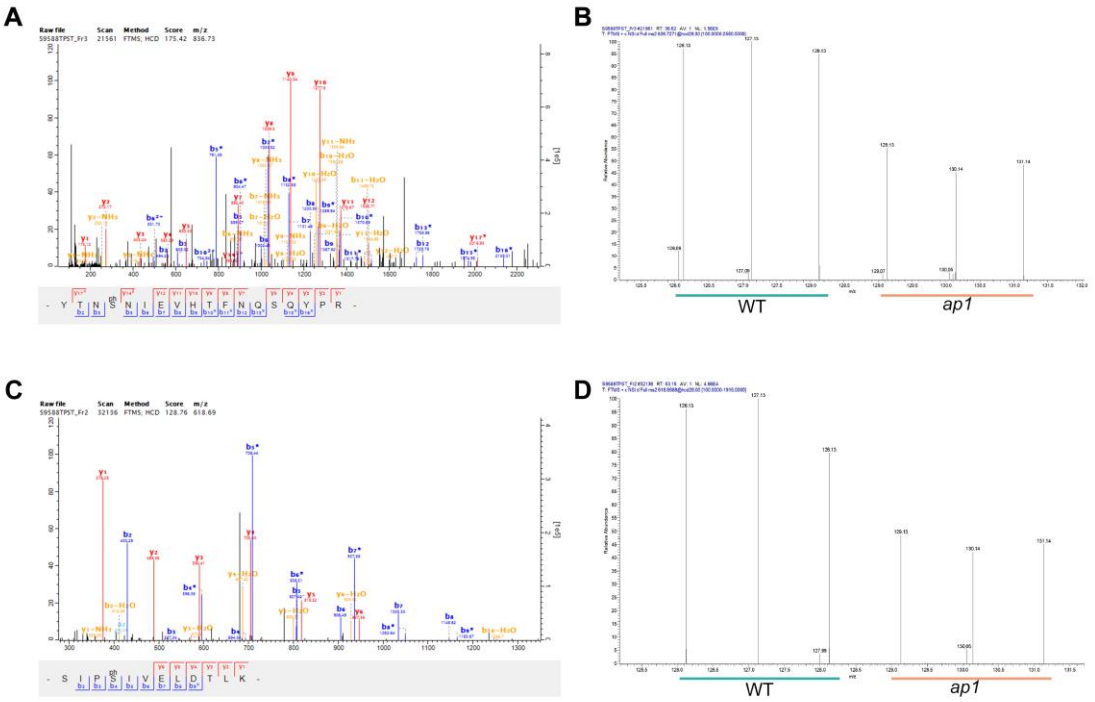

Figure S13. Representative MS/MS spectra for identification of the downregulated phosphorylation sites in OsUGP2.

(A, B) The phosphopeptide YTN**S**NIEVHTFNQSQYPR provides evidence of downregulated phosphorylation of S151. (C, D) The phosphopeptide SIP**S**IVELDTLK provides evidence of downregulated phosphorylation of S413. “b” and “y” denote peptide fragment ions retaining charges at the N-and C- terminus, respectively. The subscript numbers indicate their positions in the identified peptide.

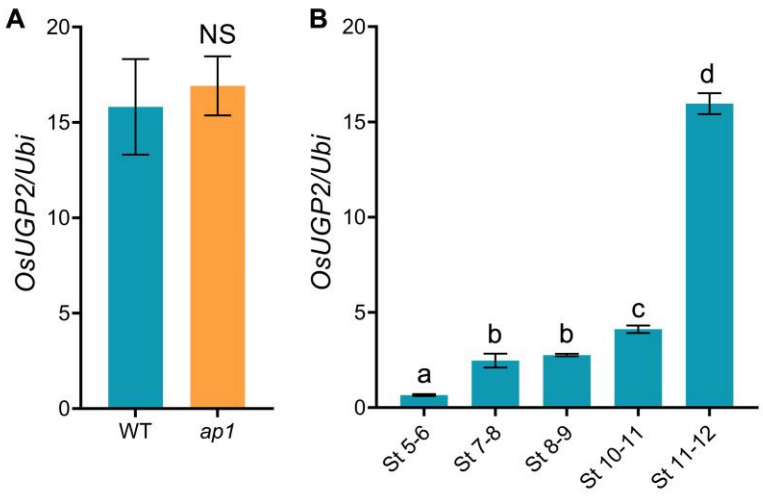

Figure S14. qRT-PCR analysis of *OsUGP2*.

(A) Expression levels of *OsUGP2* in spikelets during the anther stages 11 to 12. Values are means ± SEM of four biological replicates. NS, no significance ($P > 0.05$) compared with the WT using Student's *t*-test. (B) Expression pattern of *OsUGP2* in spikelets. RNAs were extracted from spikelets with anthers at different stages from the WT. Values are means ± SEM of four biological replicates. Statistical significance was determined by Student's *t*-test; significant differences ($P < 0.05$) are indicated by different lowercase letters.

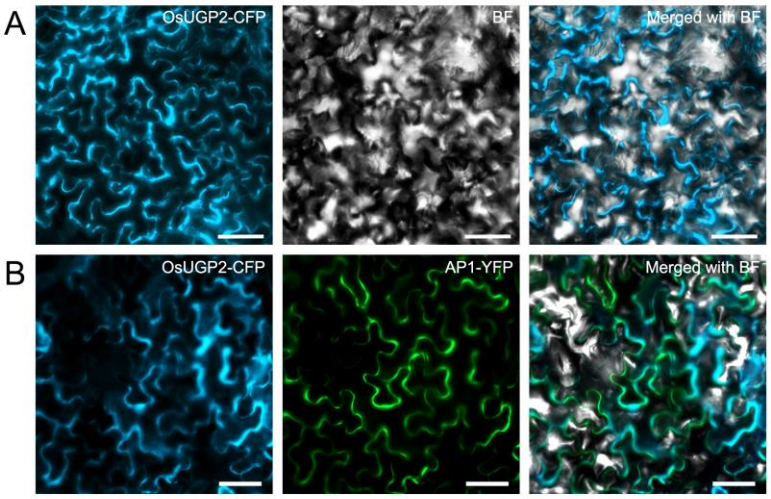

Figure S15. Co-localization of OsUGP2 and AP1 in tobacco leaf epidermis cells.

(A) Subcellular localization of OsUGP2-CFP in tobacco leaf epidermis cells. **(**B) Co-expression of OsUGP2-CFP and AP1-YFP in tobacco leaf epidermis cells. Scale bars: 50 μm.

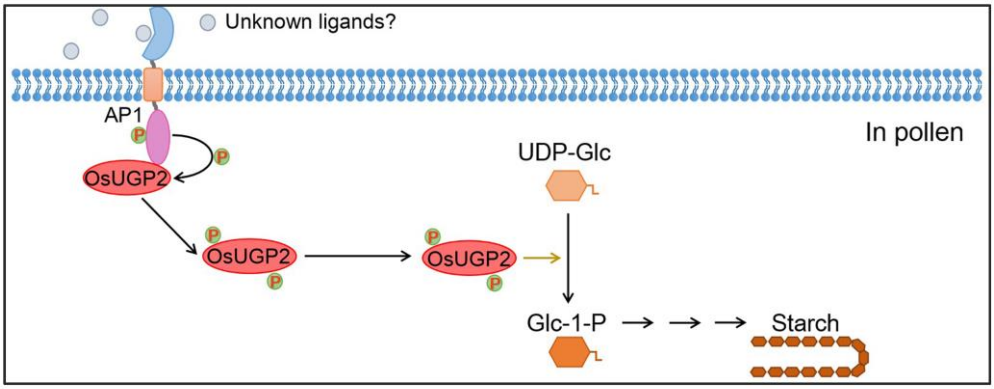

Figure S16. A proposed model for the role of AP1 in pollen starch accumulation.

In pollen, plasma membrane-associated AP1 may receive unknown signals and phosphorylate OsUGP2, which in turn promotes the pollen starch synthesis.

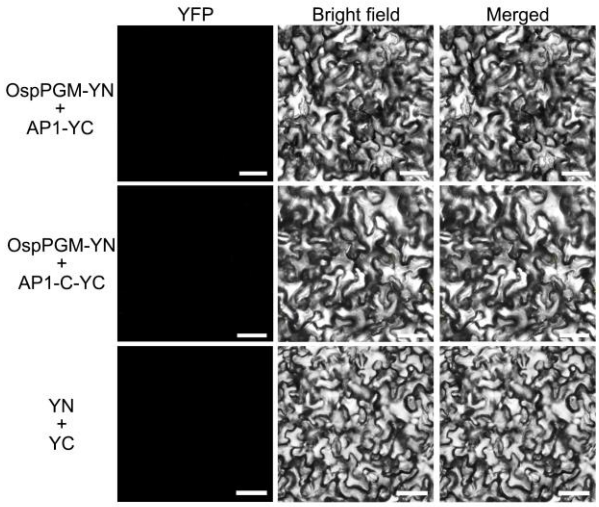

Figure S17. **AP1 could not interact with OspPGM in BiFC assays.**

Scale bars: 50μ m.

Table S1. Segregations of the F_2 population.

Phenotype or genotype	Expected	Observed	c^2	*p* value
Normal-fertility: Male-sterility	3:1	546:154	1.7522	0.1856
AP1/AP1: *AP1/ap1*: *ap1/ap1*	1:2:1	185:361:154	1.7884	0.4089

Table S2. List of SNPs with index of 1 on Chromosome 2.

Position	Base changes	Mutation type	Locus ID	Encoding protein	Effect on amino acids
12668512	A>T	Non-synonymous	*LOC_Os02g21340*	ABC-2 type transporter family protein	F330Y
13175654	G>A	Non-synonymous	*LOC_Os02g22130*	GTPase-activating protein	V113M
13288306	G>A	Intron	*LOC_Os02g22260*	Fruit protein PKIWI502	NA
15365139	C>T	Stop-gained	*LOC_Os02g26160*	Lectin receptor-like kinase	R587*
18116880	C>T	Intergenic	NA	NA	NA

NA, not applicable; *, stop codon.

Table S3. The down-regulated phosphopeptides and corresponding proteins enriched in starch and sucrose metabolism pathway.

Click here to Download Table S3

Table S4. The primers used in this study.

Click here to Download Table S4

Table S5. The unique phosphorylation sites identified from quantitative phosphoproteomic analysis

Click here to Download Table S5